4th WSEAS Int. Conf. on NON-LINEAR ANALYSIS, NON-LINEAR SYSTEMS and CHAOS, Sofia, Bulgaria, October 27-29, 2005 (pp24-29)

Indipendent Dynamics in Extended Nonlinear Networks

LUIGI FORTUNA
Dipartimento di Ingegneria Elettrica Elettronica e dei Sistemi
Università degli Studi di Catania
Viale Andrea Doria 6, 95100 Catania
ITALY

MANUELA LA ROSA
FTM - Adv. R&D NV Memories & Derivatives
Post Silicon Technologies group
STMicroelectronics, Stradale Primosole 50, 95121 Catania
ITALY

DONATA NICOLOSI
FTM - Adv. R&D NV Memories & Derivatives
Post Silicon Technologies group
STMicroelectronics, Stradale Primosole 50, 95121 Catania
ITALY

GIOVANNI SICURELLA
FTM - Adv. R&D NV Memories & Derivatives
Post Silicon Technologies group
STMicroelectronics, Stradale Primosole 50, 95121 Catania
ITALY

Abstract: - A new strategy to identify the independent dynamics of spatially extended nonlinear networks is proposed. Starting from spatial modes theory an index has been defined as the number of relevant spatial modes and therefore identifies the system degree of freedom. The proposed methodology is validated by quantifying self-synchronization in three pattern-oriented systems: bidimensional Chua's circuit arrays, Hindmarsh-Rose neurons networks and fuzzy oscillators' lattices.

Key-Words: - Nonlinear networks, Synchronization, Independent dynamics, Independent component analysis, Spatio temporal patterns, Spatial modes.

1 Introduction

When studying simulated and real-world pattern oriented nonlinear networks a fundamental problem to copy with is the definition of a meaningful measure for better characterizing and comparing the phenomena.

According to synergetic theory the emergence of patterns in complex systems can be explained by considering them as structures of coupled nonlinear subsystems that exhibit macroscopic behaviors both in time and space [1]. In the following sections spatially coherent patterns in extended nonlinear networks are investigated by assuming that spatio-temporal systems can be described using a few dominant modes [1][2]. The fundamental goal of the adopted analysis is to identify quantities representing the number of collective variables of the whole spatio-temporal behavior. In order to identify individual spatial modes in spatio-temporal systems an approach based on Spatial Independent Component (SIC) methodology is proposed. SICs recovered from data are assumed as spatial modes. Spatial modes strategy is focused on the definition of an index σ for evaluating the self-synchronization

features of extended complex systems. This index represents the number of relevant degrees of freedom which describe the temporal evolution of system spatial patterns. The proposed methodology is described in Section 2. By using various examples of spatio-temporal systems, showing emergent behaviors, the proposed approach is validated in Section 3. In particular, three case of study are reported: the first one focuses on a two-dimensional lattice constituted by Chua's circuits coupled in a regular grid; the second one investigates synchronization in Hindmarsh-Rose(H-R) bidimensional networks; finally, the proposed methodology is applied to arrays of coupled fuzzy oscillators.

2 Methodology

According to spatial modes theory, the spatial patterns exhibited at generic time *t* by distributed networks can be represented trough a linear superposition of a set of basic patterns: the so-called modes. Just few spatial modes can be used to model the system dynamics decreasing in this way the degrees of freedom of the spatio-temporal system.

Given the time series $\mathbf{X} \in \Re^{TxN}$ of a spatio-temporal system, where *T* is the number of samples and *N* the number of subsystems, it can be expanded into a set of orthonormal components $\mathbf{s}_k$ each one having a corresponding amplitude $w_k(t)$:

$$\mathbf{X}(t) = \sum_{k=1}^{N} w_k(t)\mathbf{s}_k \quad (1)$$

where t=1…*T* is the sample index.

2.1 Spatial independent component analysis

Usually, Independent Component Analysis (ICA) is used for recovering signals from a set of time acquisitions by using a linear approach [2][3] but it can also be applied to extract spatial information, that is: to identify a set of basic patterns, whose linear combination allows representing the spatio-temporal dynamics of the whole system. ICA is proposed as a method to isolate Spatial Independent Components (SICs) that can be assumed as spatial modes. Starting from the data matrix $\mathbf{X} \in \Re^{TxN}$, and being:

$$\mathbf{X} = \mathbf{W} \times \mathbf{S} \quad (2)$$

where $\mathbf{W} \in \Re^{TxN}$ is a weight matrix, the SIC analysis allows to recover *N* spatial modes, given by the matrix $\mathbf{S} \in \Re^{NxN}$. Each spatial mode is statistically independent from the others and has a non-Gaussian distribution. The matrix **S** can be evaluated by considering the estimated matrix $\hat{W}$ as follows:

$$\mathbf{S} = \hat{W}^{-1} \cdot \mathbf{X} \quad (3)$$

The algorithm to estimate $\hat{\mathbf{W}}$ is based on the estimation of the inverse of the matrix **W** obtained through a recursive algorithm. In order to identify the independent dynamics of the system we are interested in evaluating the number of spatial modes. This number, which can be up to the number of subsystems *N*, can be decreased by selecting only those spatial modes with the largest eigenvalues in the Singular Value Decomposition (SVD). In real data analysis, the highest eigenvalues are associated to the spatially coherent dynamics while the smaller ones are related to incoherent dynamics. In pattern-oriented systems, the highest eigenvalues can be associated to the spatial self-synchronized dynamics while the smaller ones can be associated to the spatially unsynchronized chaotic dynamics. The point that shows a gap from the higher to the smaller eigenvalues distribution is adopted as the number of spatial modes that identify the spatial dynamics.

2.2 Index definition

Starting from the previous considerations, an index σ [4] is proposed to identify the number of independent dynamics characterizing spatially extended system. Let's consider a generic bidimensional system constituted by interconnected units. Given the matrix $\mathbf{A} \in \Re^{NxT} \mid \mathbf{A}=\mathbf{X}^{\mathbf{T}}$, containing in its rows the *N* signals generated by the system subunits, the covariance matrix of **A** is the matrix $\mathbf{R} \in \Re^{NxN}$, $\mathbf{R} = \mathbf{A} \cdot \mathbf{A}^{\mathbf{T}}$. The index σ is a function of the eigenvalues of **R** (that are the squares of the singular values of the matrix **A**).

Depending on matrix **A** singular values, three main classes of dynamic behavior can be identified:

- Spatio-temporal chaos: all the signals are uncorrelated; in this case all the singular values are non-null and $\sigma = N$;
- Synchronization: all the signals are identical and only one singular value is non-null ($\sigma = 1$); in this case the rank of the matrix **R** will be unitary.
- Emerging patterns: the units aggregate in synchronized clusters whose number is equal to the number of spatial modes. Each cluster dynamics is identified by the relative spatial mode dynamic evolution ($1 < \sigma < N$); singular values well be both null and non-null (some very close to zero).

When signals are similar but not identical some singular values very close to zero will be found. The adopted index is thus defined at a certain percentage

ξ, as the minimum number m of eigenvalues whose sum is greater than a percentage of the trace of R:

$$\sigma(\xi) = \min m \left| \sum_{i=1}^{m} \lambda_i^{sort} > \xi \cdot Tr(R) \right. \quad (4)$$

where λ_i^{sort} is the i-th largest eigenvalue of the covariance matrix **R**. The index range of variation is $[1 \div (\xi \cdot N)+1]$ corresponding to a situation of total synchronization till a completely independent dynamics: the index is therefore an important parameter giving information about the total number of different dynamics present in the system.

3 Results

The methodology proposed has been applied investigating the spatio-temporal dynamics of three different networks: bidimensional lattices of Chua's circuits, Hindmarsh-Rose (H-R) neurons and fuzzy oscillators. The defined index allowed characterizing and comparing the networks dynamic behaviors towards the system parameter D that represents the connection strength.

3.1 Bidimensional lattices of Chua's circuits

A regular lattice has been built by connecting N=100 Chua's circuits spatially disposed on a 10x10 matrix. The single unit equations have been modified considering a nearest-neighbor coupling of radius one which behavior is described by the following equations:

$$\begin{aligned} \frac{dx_i}{dt} &= \alpha(y_i - az_i - h(x_i)) \\ \frac{dy_i}{dt} &= x_i - y_i + z_i + D\left(\sum_{j \neq i} y_j - C\ y_i\right) \quad (5) \\ \frac{dz_i}{dt} &= -\beta y_i \\ h(x_i) &= bx_i + 0.5(a-b)(|x_i+1| - |x_i-1|) \end{aligned}$$

where a=-1.27, b=-0.68, α=10 , β=14.87, C=8

The lattice collective behavior has been investigated by varying the coupling intensity D. Fig. 1 shows the time series of three generic cells of the lattice, while Fig. 2 shows the spatial patterns obtained considering four different time instants for increasing values of D by using a bidimensional 64-color map. Spatio-temporal chaos is observed for weak coupling strength ($D \in [0.1 \div 1]$), as D increases the lattice starts exhibiting emerging patterns and for values of D higher than 4 self-organization takes place and the systems conveys to perfect chaotic synchronization.

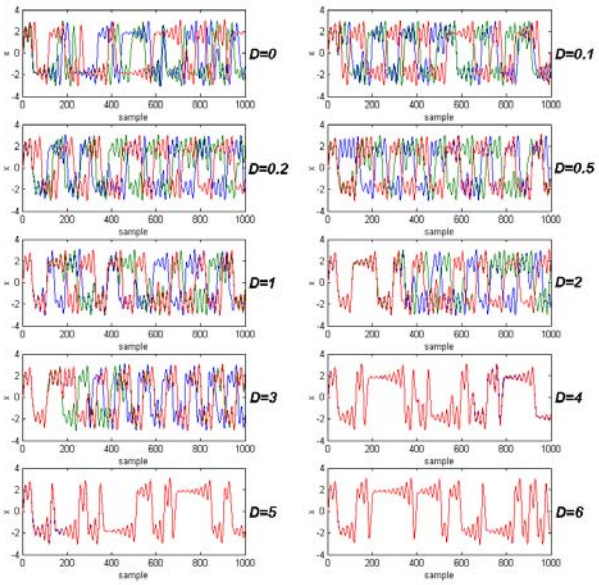

Fig.1 x variable time series for increasing values of the diffusion coefficient D of three generic circuits.

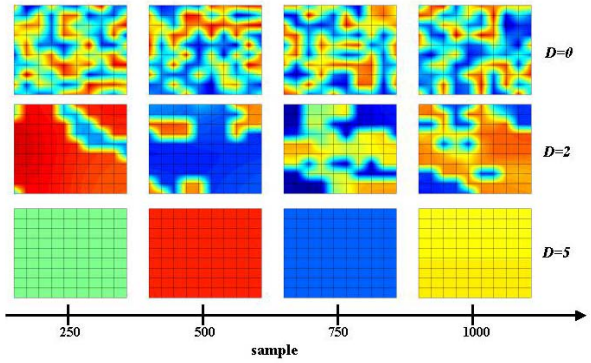

Fig.2. Bidimensional maps of 10x10 Chua's circuit lattices for different values of D.

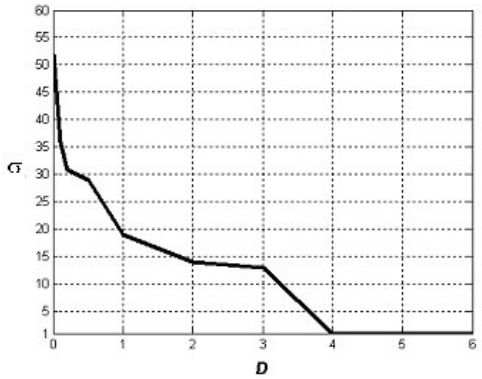

Fig. 3. σ vs. D in a 10x10 lattice of Chua's circuits.

The defined index has been then evaluated for increasing values of D. Coherently with the previous results, a value of σ has been associated to the dynamic evolution of the lattice characterizing then the system synchronization degree versus the coupling D, as is it shown in Fig. 3.The index σ

decreases as the coupling strength increases: it is maximum for $D = 0$, when all the circuits are disconnected and spatio-temporal chaos is shown. For small values of $D \in [0.1 \div 1]$, the index value becomes smaller and emerging patterns arise. Then, for values of D greater than 4, the index σ becomes equal to 1 and the perfect chaotic synchronization is reached: the system constituted by $N=100$ cells behaves as a whole and only one dynamic evolution can be isolated.

3.2 Bidimensional network of H-R neurons

A bidimensional network of N=100 Hindmarsh-Rose neurons [5] is built by disposing each unit on a 10x10 array with radius one. The lattice dynamics is defined by equations (6), where C=8 is the number of connected cells and i=1÷100, r=0.0021, S=4, I=3.281.

$$\begin{aligned} \frac{dx_i}{dt} &= y_i + 3x_i^2 - x_i^3 - z_i + I_i + D\left(\sum_{j\neq i} x_j - Cx_i\right) \\ \frac{dy_i}{dt} &= 1 - 5x_i^2 - y_i \\ \frac{dz_i}{dt} &= -rz_i + rS(x_i + 1.6) \end{aligned} \qquad (6)$$

The state-variables $x(t)$ and $y(t)$ model the fast dynamics while $z(t)$ models the slow one; variable I represents the synaptic current. The coupling strength D weights the coupling between the i-th neuron and its neighbors. Model parameters have been set in such a way that each isolated neuron is characterized by a chaotic behavior, each of them starting from random initial conditions. In Figg.4 and 5 the membrane potentials x of three coupled neurons and the bidimensional maps of the lattice, respectively, are displayed for increasing values of D.

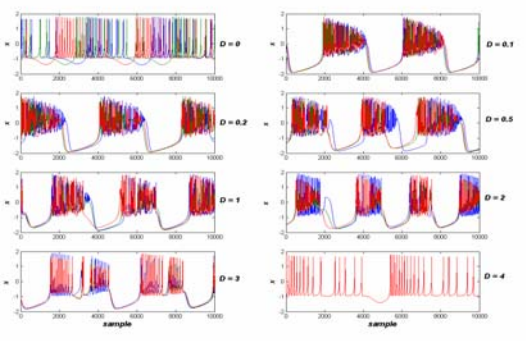

Fig.4 x variable time-series for different values of the diffusion coefficient D of three generic neurons.

As shown in Fig. 4, the system is characterized by two different regimes, slow and fast, requiring a different and accurate analysis. In the uncoupled case, when D=0, the potentials $x(t)$ evolve independently and the maps, displayed for different time instants, present isolated spots underlining the uncorrelated evolution of each neuron. In case of weak couplings, when $D \in [0.1 \div 2]$, the neurons evolve with slow periodic dynamic and fast unsynchronized spikes; as shown in Fig. 5, spatio-temporal patterns arise. The dynamics changes for stronger couplings, when D>3: in this case, the neurons are chaotically synchronized as shown in Figg. 4 and 5. When the perfect synchronization is obtained both burst slow activities and spike fast regime become synchronized: the 100 neurons behave as an individual chaotic one and the 64-color maps obtained for fixed time instants have a homogeneous color.

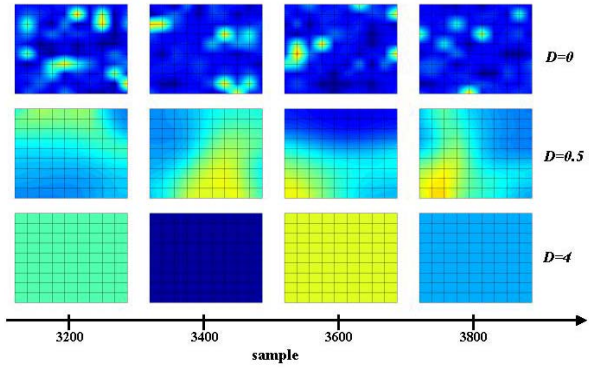

Fig.5 Bidimensional maps of 10x10 Hindmarsh-Rose neuron networks for different values of D.

The spatio-temporal behavior of the H-R lattice has been then investigated trough the proposed index σ. Starting from weak couplings, the synchronization index is far from 1, as shown in Fig. 6.

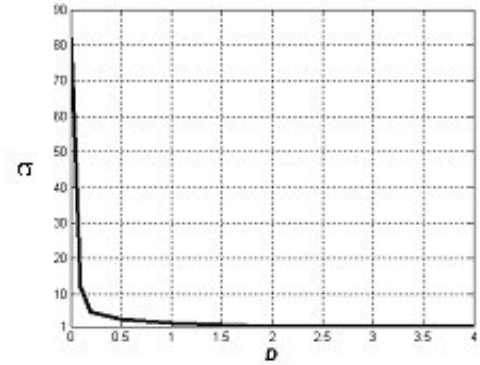

Fig.6 σ vs. D in a 10x10 network of H-R neurons.

The σ vs. D curve appears very steep and decreases suddenly for higher values of the coupling strength D. The network self-organization, quantified according to the perfect synchronization of both slow and fast regimes, respectively burst and spikes

dynamics, is obtained for a diffusion coefficient D higher than 3 when σ =1, as reported in Fig. 6. The obtained results confirmed the close relationship between synchronization performances and adopted measure.

3.3 Fuzzy oscillator lattice

A discrete chaotic fuzzy oscillator is the fundamental unit [6]. This fuzzy system is obtained through a linguistic description of the stretching and folding features in relation to an assigned value of the Lyapunov exponent. The single oscillator is described by the two variables x and d that are respectively the nominal value of the state and the uncertainty on the center value. These variables generate the desired evolution and perform the stretching and folding features. The discrete fuzzy oscillator dynamic could be considered like a two dimensional chaotic map with the following structure:

$$x(k+1) = \Psi\ (x(k), d(k)) \qquad (7)$$
$$d(k+1) = \Phi\ (x(k), d(k))$$

where Ψ and Φ are the fuzzy inference functions described through a set of fuzzy rules for each variable, as reported in Table 1. The ranges of the variables are chosen according to a suitable embedding zone performing a main oscillatory dynamics summed to an uncertain evolution. The design of the fuzzy sets, shown in Fig.7, is obtained by fixing a desired Lyapunov exponent l. In Fig. 8, the chaotic time series generated by a fuzzy oscillator with l=0.1 is shown.

x(k)/d(k)	zero	small	large	verylarge
x.large.left	x.small.left/zero	x.small.left/medium	x.small.left/verylarge	x.small.right/large
x.small.left	x.large.left/zero	x.large.left/medium	x.large.left/verylarge	x.large.left/small
x.small.right	x.large.right/zero	x.large.right/medium	x.large.right/verylarge	x.large.right/small
x.large.right	x.small.right/zero	x.small.right/medium	x.small.right/verylarge	x.small.left/large

Table 1 Rules of the adopted fuzzy inference system.

The lattice configuration is set with a regular distribution of the connections with a ring topology that means that each unit has $2 \cdot C$ neighbors half on the right and half on the left. The equations describing the system of N oscillators are reformulated in (8) where D represents a suitable diffusion coefficient related to a desired information exchange.

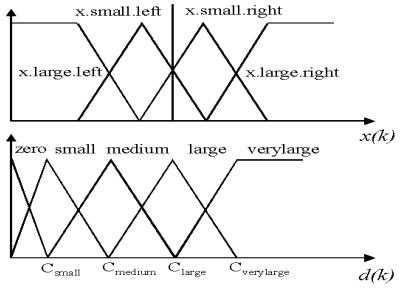

Fig.7 Fuzzy sets of the discrete fuzzy chaotic oscillator.

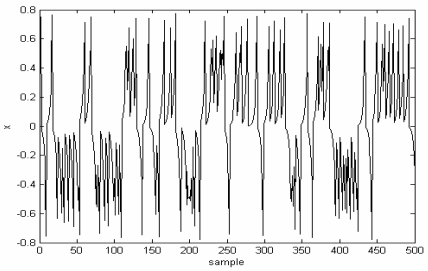

Fig.8 Time series of a fuzzy oscillator with Lyapunov exponent equal to 0.1.

$$x_i(k+1) = \Psi\left(x_i(k) + D\left(-2Cx_i(k) + \sum_{\substack{j=-C \\ j\neq 0}}^{C} x_{i+j}(k) \right),\ d_i(k) \right) \qquad (8)$$
$$d_i(k+1) = \Phi(x_i(k), d_i(k)) \qquad i = 1..N$$

The state value of each fuzzy oscillator depends on its own state value in the previous sample time and on the contributions coming from the state values of the other fuzzy oscillators connected, through a bidirectional information exchange. A lattice of N=200 discrete fuzzy chaotic oscillators with l= 0.1 has been considered, with a constant diffusion coefficient D=0.005. The single-unit starts its evolution from random initial conditions. Fig.9, shows the spatio-temporal maps obtained for different values of C; in the x-axis is indicated the time in sample, while in the y-axis is reported the index associated to each cell (i). The state value x_i of the i-th cell is represented through the colors. By varying the number of connections per unit four different global dynamics are observed: an initial condition characterized by spatio-temporal chaos for C=4, two types of synchronization (regular for C=16 and chaotic for C=46) and a transition phase for C=25. In Fig. 10 in order to explain the meaning of these different spatio-temporal dynamics the nominal value x_i of the i-th cell (for i=100 and i =101) is displayed. For C=4 each chaotic oscillator evolves with its own dynamics (Fig. 10a); for C=16 regular oscillations are visible (Fig. 10b); for C=25 the two cells time evolutions become almost the same in long

time intervals (Fig. 10c); for C=46 a chaotic synchronized behavior is obtained (Fig.10d).

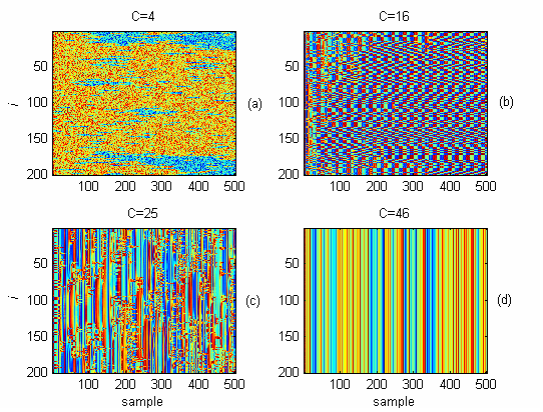

Fig.9 Spatio-temporal maps of fuzzy lattices with: C=4 (a), C=16 (b), C=25 (c), C=46 (d).

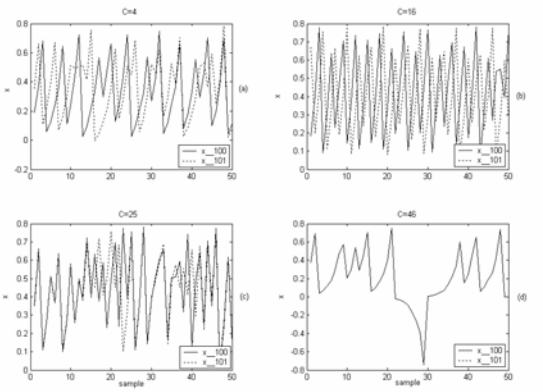

Fig.10 x variable time series of two cells in fuzzy lattices with: C=4 (a), C=16 (b), C=25 (c), C=46 (d).

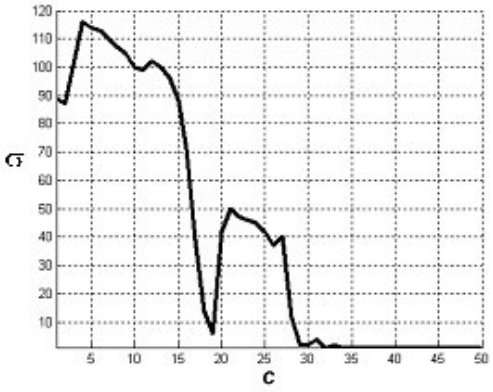

Fig.11 σ vs. C in regular fuzzy oscillators arrays with Lyapunov exponent l=0.1.

The results of this analysis have been validated by using the spatial mode approach. The index σ has been evaluated for the lattice of N=200 fuzzy oscillators with Lyapunov exponent l=0.1 and a regular distribution of the connections. The values of σ versus C are reported in Fig.11: the presence of two zones underlines a transition between two synchronization phases of the array dynamics. The spatio-temporal behaviors reported in Fig. 9a and Fig. 9c show unsynchronized evolutions of the fuzzy oscillator arrays. However, visually inspecting the two maps, the one in Fig. 9c shows to have a higher spatial coherence. This conjecture is quantitatively validated by the evaluated index σ. For C=4, σ has the maximum value (σ =115) while for C=25 the index value is σ =41.

4 Conclusion

The introduction of a synchronization index, allows quantifying the self-organization level of an extended network and evaluating its behavior versus structural parameters. The introduction of this value allows quantifying the self-organization level of an extended network and evaluating its behavior versus structural parameters. Moreover, by identifying the reference spatial modes and their corresponding time-dependent evolution, the real dynamics of the system is separated from noise and the number of its independent dynamics is quantified. The proposed methodology has been applied to several spatio-temporal networks. The suitability of the proposed measure in order to quantify the various dynamics of pattern-oriented networks has been proved.

Acknowledgements:
The activity has been partially supported by the Italian "Ministero dell'Istruzione, dell'Università e della Ricerca" (MIUR) under the FIRB Project RBNE01CW3M_001.

References:

[1]H. Haken, *Synergetics. An Introduction*, Springer, 1983.

[2]M. Bucolo, L. Fortuna, M. Frasca, M. La Rosa, D. S. Shannahoff-Khalsa, L. Schult, J.A. Wright, Independent Component Analysis of Magnetoencephalography Data, *In Proc. 23rd EMBC*, 2001.

[3]A. Hyvarinen, E. Oja, Independent Component Analysis: algorithms and applications, *Neural Networks*, Vol. 13, 2000, pp.411-430.

[4]S. Cosenza, P. Crucitti, L. Fortuna, M. Frasca, M. La Rosa, C. Stagni, and L.Usai, From Net Topology To Synchronization in HR Neuron Grids, *Mathematical Biosciences And Engineering*,Vol. 2, No. 1, 2005.

[5]J. L. Hindmarsh, R. M. Rose. *Proc. R. Soc. London B*, 221(1984) 87.

[6]G. Manganaro, S. Baglio, L. Fortuna, Design of Fuzzy Iterators to Generate Chaotic Time Series with Assigned Lyapunov Exponent, *Electronic Letters*, Vol. 32, 1996.